View metadata, citation and similar papers at core.ac.uk
brought to you by CORE
provided by Electronic Sumy State University Institutional Repository

JOURNAL OF NANO- AND ELECTRONIC PHYSICS
Vol. 5 No 4, 04060(6pp) (2013)

ЖУРНАЛ НАНО- ТА ЕЛЕКТРОННОЇ ФІЗИКИ
Том 5 № 4, 04060(6cc) (2013)

Development of the RF Ion Sources for Focused Ion Beam Accelerators

V. Voznyi*, V. Miroshnichenko, S. Mordyk, D. Shulha, V. Storizhko, V. Tokman

Institute of Applied Physics, National Academy of Sciences of the Ukraine,
58, Petropavlovskaya Str., 40000 Sumy, Ukraine

(Received 26 June 2013; published online 31 January 2014)

The paper presents the results of investigations of ion sources developed in the IAP of NAS of Ukraine for generation of high brightness ion beams with small energy spread. A series of RF ion sources operated at the frequency of 27.12 MHz were studied: the inductive RF ion source, the helicon ion source, the multicusp RF ion source, and the sputter type RF source of metal ions. A global model and transformer model were applied for calculation of RF source plasma parameters. Ion energy spread, ion mass, and ion current density of some sources were measured in the wide range of RF power, extraction voltage and gas pressure.

Keywords: RF ion source, Plasma, Inductive, Helicon, Multicusp, Sputtering.

PACS numbers: 41.75.Ak, 52.50.Qt, 52.80.Pi

1. INTRODUCTION

The focused ion beams (FIB) accelerators are widely used in semi-conducting industry and materials science. Radio-frequency (RF) ion sources are usually equipped with the FIB accelerators providing spatial resolution of about 1μm [1]. Chromatic d_c and spherical d_s aberrations of electrostatic lenses induce beam broadening and depend on the beam brightness B_p and beam energy spread ΔE as follows: $d_c \sim B_p^{-1/4}$, $d_c \sim \Delta E / E$, и $d_s \sim B_p^{-3/8}$ [2]. The brightness B_p of an ion source is defined as $B_p = I / (S\Omega E)$, where I is the ion current, S is the emission area, Ω is the beam divergence angle, E is the beam energy [3]. From these formulae it is obvious that the spatial resolution of the FIB accelerators may be improved and transferred to a submicron range of measurement by application of ion sources with high brightness and high ion current density.

FIB machines are widely used in micro-and nanotechnologies, in particular, in fabrication of various micro-devices of micron size. Focused Ion Beam milling is one of the basic methods for nanomaterials shaping. A material is removed by a focused ion beam of an energy sufficient to knock an atom out of a detail surface. Argon is used here as a source of projectile ions. Used for ion milling the plasma RF ion sources can compete with commercial sources like duoplasmatron and liquid-metal ion source, since it offers several advantages as absence of a heated cathode, pure plasma creation, ability to operate with reactive gases. To increase the performance of the ion milling it is necessary to use ion sources with a high current density and a high brightness. The main ion source parameter that determines a speed of ion treatment is the ion current density. Thus, the efficiency of the FIB machine may be increased by ion sources of high ion flux density and high brightness.

Recently the experiments became more significant on studying the structural materials for nuclear technology radiated by charged particles beams in order to simulate changing of the material properties occurred when operating with nuclear materials. Such simulations are possible with ion metal beams accelerated up to energy initiating a number of atoms shifts in a material matrix similar to that of structural materials operated.

The paper presents the results of studying of the ion sources [4-13] designed in the Institute of Applied Physics, Sumy, Ukraine for solving of these problems. A series of RF ion sources operated at the frequency of 27.12 MHz are considered: an inductive RF ion source without external magnet field, a helicon RF in longitudinal magnetic field, a multicusp RF ion source with an internal antenna, and a sputter type RF source of metal ions.

2. INDUCTIVE RF ION SOURCE

The inductive RF ion source without magnetic field [5, 11, 13] is schematically shown in Fig. 1. A cylindrical quartz discharge tube with a diameter of 30 mm and the length of 70 mm is wound with 4 turns of a coil of RF antenna. The coil is supplied with the RF power up to 300 W and frequency of 27.12 MHz. The RF current induces an electromagnetic field whose energy is absorbed by plasma electrons.

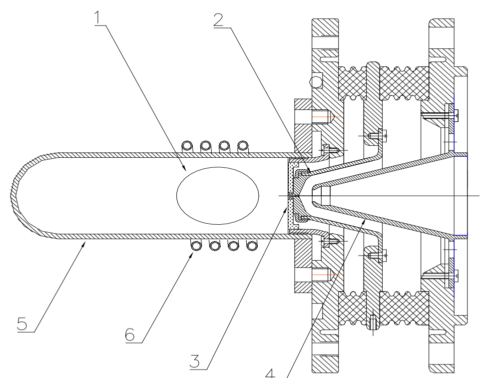

Fig. 1 – Diagram of the inductive RF ion source: 1 is plasma volume, 2 is an extractor, 3 is a diaphragm, 4 is a focusing electrode, 5 is a quartz tube, 6 is a coil of a RF antenna

* vozny@ipflab.sumy.ua

© 2013 Sumy State University

2.1 The Transformer Model

The transformer model [14, 15] of an inductive RF discharge was applied for measuring the RF power absorbed by the plasma of ion source. Here an RF antenna and a discharge form an air-cored transformer with an RF antenna as a primary winding, and plasma as a one-turn secondary winding. The external electrical characteristics of the RF circuit – the current and the voltage at the antenna - were measured in RF power range of 10-400 W and a gas pressure of 0.1-4 Pa [11]. The results measurements were used for determination of inner parameters of the RF discharge as RF efficiency, azimuthal plasma current, efficient frequency of electron-neutral collisions, plasma resistance.

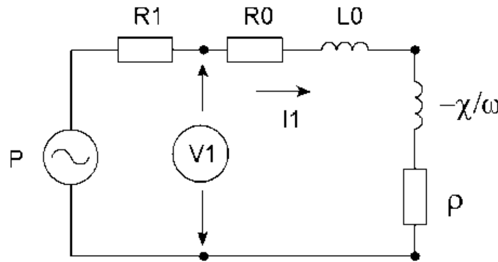

Fig. 2 - Equivalent series circuit of the transformer model

In the transformer model a coupled RF circuit can be transformed into a series circuit (Fig. 2). Plasma load is regarded as addition of equivalent plasma resistance ρ and equivalent plasma inductance χ. The power P induced by an RF generator is the sum of the power dissipated in the coupling circuit P_1 and in the antenna P_{ant} and the power absorbed by the plasma P_{abs}: $P = P_1 + P_{ant} + P_{abs} = I_1^2(R_1 + R_0 + \rho)$. Loss resistance $(R_1 + R_0)$ is found by measuring the antenna current I_0 and delivered power P in no plasma condition: $R_1 + R_0 = P / I_0^2$. The power efficiency is defined as: $\eta = P_{abs} / P = 1 - (R_1 + R_0)I_1^2 / P$. Fig. 3 shows the dependence of the power efficiency η on delivered RF power P at different argon pressure.

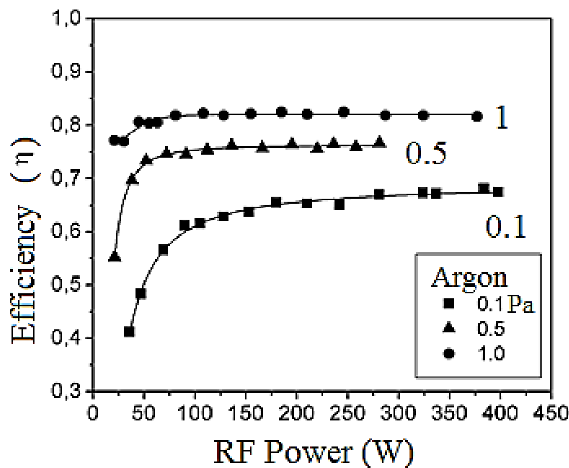

Fig. 3 - Power efficiency vs delivered RF power at different argon pressure

The transformer model calculations showed that electrodeless azimuthal plasma current reaches 30 A at 400 W of RF power and is N times higher than the antenna current, where N is a number of turns of the coil. Active resistance of plasma equals a few Ohms and decreases as RF power grows [16]. It is due to RF field penetration depth being inversely proportional to square root of plasma density. The discharge behavior at high plasma density corresponds to a transformer with a shorted secondary winding.

2.2 The Global Model

The global model of plasma discharge [16] is applied for determination of the plasma density n_e, the electron temperature T_e and the ion current density j_s that can be extracted from the plasma source. The electron temperature T_e is defined from the particles balance equation. Loss of the electrons and ions at the surface of the discharge chamber is balanced by electron-ion pairs formed at ionization in the plasma volume [16]: $K_{iz}(T_e) / u_B(T_e) = 1 / n_g d_{eff}$, where K_{iz} is the kinetic coefficient of neutrals ionized by electrons, $u_B = (kT_e / M)^{1/2}$ is the Bohm ion velocity, k is the Boltzmann constant, M is the ion mass, n_g is the neutral gas density. The effective plasma dimension d_{eff} is defined as $d_{eff} = 0.5RL / (Lh_R + Rh_L)$, where R, L are the radius and length of the discharge, h_R and h_L are geometric factors.

Calculations showed that the electron temperature depends on the argon pressure and the discharge dimensions R, L and is independent from the plasma density and thus from the absorbed RF power [5, 13]. The electron temperature goes down as the pressure increases and for $D = 2R = 30$ mm and $L = 70$ mm $T_e = 3$ eV at 1 Pa (7.5 mTorr).

The mean plasma density is defined from the power balance equation in the discharge. The power absorbed by the discharge goes for generation of the electron-ion pairs including all elastic and inelastic collisions (ionization, excitation) in the volume. The rest part of the power is lost as kinetic energy of the ions and electrons as they hit the chamber walls. The full power balance is [16]: $P_{abs} = n_s u_B A \varepsilon_T$, where P_{abs} is the power absorbed by the plasma, n_s is the plasma density at the discharge chamber wall, A is the area of the discharge chamber, ε_T is the total energy lost per ion. From this equation we can obtain an average plasma density: $n_e = P_{abs} / u_B A_{eff} \varepsilon_T$, where $A_{eff} = 2R(Lh_R + Rh_L)$.

The dependence between the mean plasma density n_e and argon pressure p and absorbed RF power was defined as $n_e = 1{,}57 \cdot 10^{16}\, p^{0.4} \cdot P_{abs}$, where n_e is expressed in m^{-3}, p in Pa, P_{abs} in W. The mean plasma density is proportional to RF power and increases with gas pressure. Calculated plasma density is in good agreement with the microwave interferometer measurements that speaks for validity of this technique in plasma parameters calculations for a RF ion source.

The maximum ion current density that can be extracted from the plasma source – a saturation current density j_s – depends on the plasma density and electron temperature as [16]: $j_s = en_s u_B = en_e h_L (kT_e / M)^{1/2}$.

Ion current density of argon beam was calculated for different dimensions of discharge chamber $D = 2R$ and L of ion source as function of argon pressure (Fig. 4). It is found that ion current density grows at decrease of the chamber dimensions. For $D = 30$ mm

and $L = 70$ mm the ion current density is 23 mA/cm^2 at $P_{abs} = 100$ W. The ion current density increases up to $j_s = 40$ mA/cm^2 at the flask length of 35 mm. As the discharge chamber length decreases up to 15 mm the ion current density can achieve 85 mA/cm^2 at 100 W of absorbed RF power [13].

The ion current density was measured as a function of extraction voltage V_{ext}. It was found that ion current density increases as extraction voltage grows and it reaches a saturation at $V_{ext} = 2.4$ kV. At RF power of $P_{abs} = 120$ W and the argon pressure of $p = 0.9$ Pa the maximum ion current density is equal to 43 mA/cm^2 and is in good agreement with the value of 40 mA/cm^2 calculated using the global model [13].

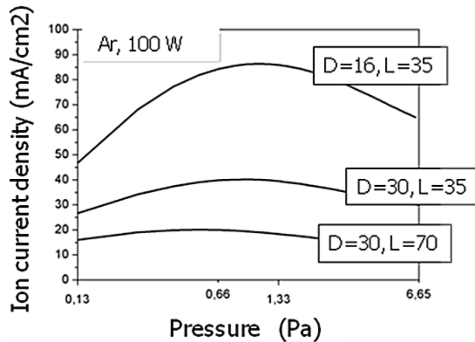

Fig. 4 - Saturation ion current density j_s as function of argon pressure for different dimensions D, L of a discharge chamber

3. INDUCTIVE RF ION SOURCE IN LONGITUDINAL MAGNETIC FIELD

Since in RF ion source the plasma frequency ω_{pe} is greater than the working frequency ω, the electromagnetic field excited by the RF antenna cannot penetrate deep into the plasma. Electromagnetic energy is transferred to plasma electrons in a skin-layer having the depth inversely proportional to square root of the plasma density: $\delta_p = c / \omega_{pe} = (m_e / \mu_0 n_e e^2)^{1/2} = 5.3 \cdot 10^6 / n_e^{1/2}$, where c is the light velocity, m_e is the electron mass, μ_0 is the magnetic constant, e is the electron charge. It is seen that as RF power increases and plasma density increases as well, a skin depth decreases and electromagnetic energy transfer to plasma becomes difficult. It may be overcome by placing the discharge chamber of the ion source in the external longitudinal magnetic field. In this ion source called a helicon source the magnetic field facilitates excitation of the electromagnetic waves whose energy penetrates into the plasma and is absorbed in whole plasma volume [17, 18]. A plasma cylinder in axial magnetic field is a resonant cavity in which eigenmodes are excited. There are two modes in a low-frequency range (10-100 MHz): electromagnetic helicon wave (H-wave) and electrostatic wave (TG-wave); dispersion relations of the two branches of the oscillations are [19, 20]: $\omega = (\omega_{ce} k_z k c^2 - j\nu_e k^2 c^2) / \omega_{pe}^2$, $\omega = \omega_{ce} k_z / k - j\nu_e$, where ω_{ce} is electron cyclotron frequency; ν_e is frequency of electron-neutral collisions; k_z, k_r and k are longitudinal, transverse and total wave numbers; j is the imaginary unit. The RF antenna excites helicon wave weakly absorbed by the plasma. The helicon wave, in turn, excites the TG-wave, whose energy is well absorbed by the plasma in electron-neutral collisions. Since a beam emittance increases as magnetic field grows up, low magnetic field is to be applied to obtain a beam of a high brightness. With magnetic field decreased, helicon mode gradually decays; at a magnetic field when electron cyclotron frequency ω_{ce} is twice as high as the operating frequency ω ($\omega_{ce} \sim 2\omega$), only electrostatic TG-wave being an electron-cyclotron wave in the bounded cylinder propagates in the plasma. The electron-cyclotron resonance occurs at $B \approx 20$ G for working frequency of 27.12 MHz.

The ion current density of the argon beam of the helicon ion source has been measured in the magnetic field $B \approx 20$ G created by the ring permanent magnets [4, 6, 7, 10, 12]. The RF antenna consists of 3 winding of copper tube and is azimuthally symmetric helical antenna. Fig. 5 shows the dependence of the ion current density on extraction voltage at $B = 20$ G and $B = 0$. Ion current density reaches value of 100 mA/cm^2 at 120 W of RF power. This value is several times higher than the ion current density from RF source in the absence of the external magnetic field.

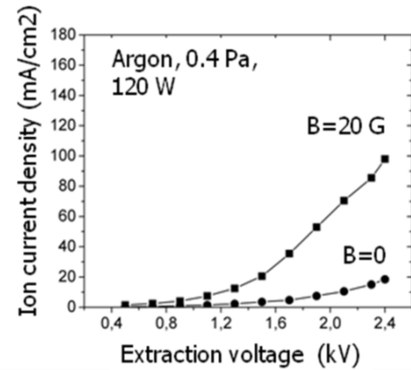

Fig. 5 - Ion current density as a function of extraction voltage at $B = 20$ G and $B = 0$

4. MULTICUSP RF ION SOURCE

A multicusp RF ion source have been designed to obtain an ion beam with a small ion energy spread [6, 8, 9]. The source consists of a cylindrical metal chamber of 47 mm in inner diameter 80 mm in length (Fig. 6). The external surface of the chamber is surrounded by a number of permanent Nd-Fe-B magnets placed with variable polarity, generating a cusp magnetic field configuration. External multicusp field confines plasma magnetically and isolated it from the discharge chamber walls, thus increasing plasma density. The magnetic field is 0.3 T near the wall and weakens the centre of the discharge chamber.

The RF antenna is placed in the discharge chamber center of free from a magnetic field. The antenna is made of a flexible copper wire threaded inside a glass tubing and is water-cooled.

A grid energy analyzer was applied for ion energy distributions (IEDF) of Ar and He beams to be measured as function of extraction voltage, gas pressure and RF power with the retarding potential method [9]. Fig. 7 shows the change of the energy distribution of the Ar ion beam as function of gas pressure. The ion energy spread ΔE was determined as function of gas

pressure and RF power by measuring the IEDF width at its half-height. It is found that the ion energy spread does not depend on gas pressure and grows with increase of RF power. At $P = 200$ W the minimal ion energy spread is equal to $\Delta E = 8$ eV for the He beam and to $\Delta E = 11$ eV for the Ar beam.

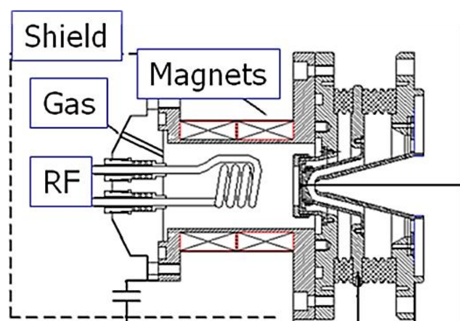

Fig. 6 - Scheme of the RF multicusp ion source

The main parameter that determines the shape of the IED is the ratio $\beta = \tau / \tau_{RF}$, where τ is the time of ion passing the sheath of a space charge in an extraction zone; τ_{RF} is the RF period. At $\beta << 1$ the ions cross the sheath over a small part of an RF cycle. Their energy depends on phase of RF oscillations; it is averaged and strongly modulated. This results in a significant broadening of the IEDF which is two-peaked. The two peaks correspond to the minimum and maximum value of the RF voltage amplitude. A two-peak structure of the IEDF at low gas pressure indicates the presence of capacitor coupling of the RF-discharge with an extracting electrode.

At $\beta >> 1$ the RF potential changes repeatedly while the ion passes the sheath of space charge. The phase of RF cycle the ion enters the sheath with becomes of no importance. As a result, the width of the IEDF decreases and two peaks approach each other until they already cannot be resolved [21]. The multipeak structure of the IEDF at high gas pressure indicates the ion scattering and resonant charge exchange at ion passing the sheath (Fig. 7).

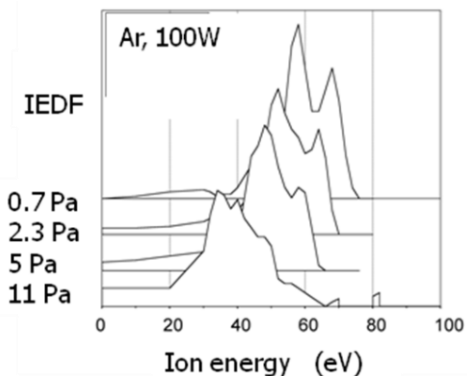

Fig. 7 - Evolution of ion energy distribution function with increasing argon pressure

The ion current density of the Ar beam have been measured. At RF power of 200 W the ion current density is equal to 55 mA/cm^2.

5. SPUTTER TYPE RF SOURCE OF METAL IONS

Simulation experiments on studying the structural materials for nuclear technology radiated by charged particles beams require metal ion beams. Ability to produce of Cu^+, Ti^+ ion beams using RF sputtering is shown in [22], and of Fe^+ beams is in [23]. In development of a RF source of Fe, Cu, Ni ions in the IAP NAS of Ukraine it was decided to use a design of a multicusp RF source with an internal antenna and to accessorize it with a sputtering target. A metal chamber of the ion beam source is 47 mm in internal diameter and 80 mm in length (Fig. 8). The water-cooled RF antenna is a cylindrical coil 30 mm in diameter made of 5 winding of a 3 mm copper tube. The target is a rod 6 mm in diameter made of required metal (Fe, Cu, Ni), being located in the center of the antenna.

A 60 MHz RF voltage is supplied to the antenna from a 300 W push-pull self-oscillator. Argon is filled into the source chamber up to 40 Pa. At a certain RF power an inductive discharge is ignited in the chamber and Ar plasma is created. A red-purple light is observed through a chamber view port. As a negative voltage $U_t = 1$ kV with discharge current about $I_t = 40$-60 mA is applied to the target, the metal target is heated up to a melting temperature, intensively sprayed and evaporated. Plasma glow gets very bright blue color when Fe is sputtered and green color when Cu is sputtered. Vaporized metal atoms are ionized in plasma region, extracted and formed into a beam of metal ions.

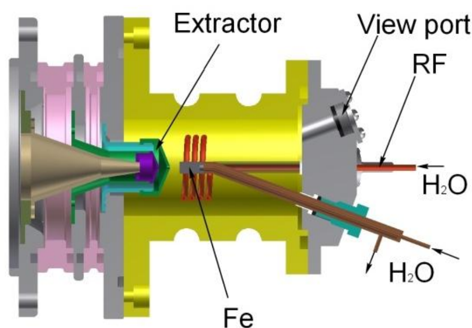

Fig. 8 - Scheme of RF source of metal ions

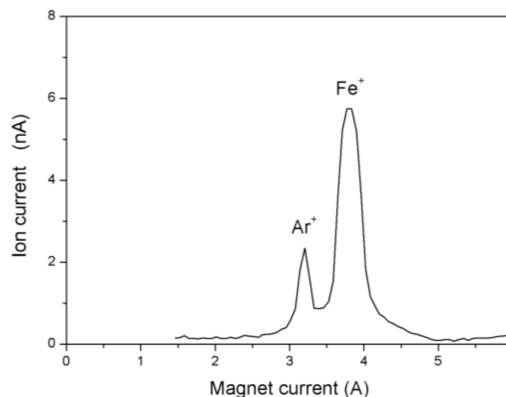

Fig. 9 - Mass-spectrum of ion beam source with a Fe target. $U_t = 1.08$ kV, $I_t = 60$ mA, $p = 40$ Pa, $I_i = 12$ µA

Measurements of the total ion current and mass composition of the ion beam were carried out. The beam mass spectrum was measured using a Wien filter.

Fig. 9 shows a mass-spectrum of ion beam source with a Fe target. Only two peaks of the Ar^+ and Fe^+ singly charged ions are seen in the spectrum and Fe^+ ion peak is three times higher than Ar^+ peak. The total ion current I_i is equal to 12 μA at ~ 250 W of RF power and 40 Pa of argon pressure. Thus at these condition the Fe^+ ion current is about 10 μA.

6. CONCLUSION

The paper considers the ion sources developed in the Institute of Applied Physics National Academy of Science of Ukraine to improve the resolution of FIB machines. Study of the plasma RF-sources was aimed to determine the conditions when the source generates a beam with a high ion current density and small energy spread. Applying a global model and a transformer model allowed the plasma density, the electron temperature, and the ion current density of the inductive RF ion source to be determined. Ion current density of the inductive and helicon RF sources and energy spread of a multicusp RF source were measured. It was found that at 120 W of delivered RF power the helicon ion source provides high current density of 100 mA/cm^2, while a multicusp RF source is characterized by a minimum energy spread of about 7 eV at the same power.

A sputter type RF source of Fe^+, Cu^+, Ni^+ ion beams was designed for experiments on studying the effect of irradiation of structural materials by charged particle beams. At ~ 250 W of RF power and 40 Pa of Ar pressure the ion current of Fe^+ ions about 10 μA has been obtained.

ACKNOWLEDGMENTS

The authors acknowledge the assistance of Mrs. H. Torchylo with the translation and preparation of this paper for publication.

The work is done in accordance with the plan of scientific research within the Ukraine state budget scientific subject 0105U000494 and 0107V000312.

Разработка ВЧ ионных источников для ускорителей сфокусированных ионных пучков

В.И. Возный, В.И. Мирошниченко, С.Н. Мордик, Д.П. Шульга,
В.Е. Сторижко, В.В. Токмань

Институт прикладной физики, Национальная академия наук Украины,
ул. Петропавловская, 58, 40000 Сумы, Украина

Представлены результаты исследований ионных источников, разработанных в ИПФ НАН Украины, для получения высокояркостных ионных пучков с малым энергетическим разбросом. Проведено исследование ряда ионных ВЧ-источников, работающих на частоте 27,12 МГц: индуктивного ВЧ-источника, геликонного источника, мультикаспового ВЧ-источника и распылительного ВЧ-источника ионов металлов. Для расчета плазменных параметров ВЧ-источников рассматривалась глобальная и трансформаторная модели разряда. Проведены измерения энергетического разброса, массового состава и плотности тока некоторых источников в широком диапазоне ВЧ-мощности, вытягивающего напряжения и давления рабочего газа.

Ключевые слова: ВЧ источник ионов, Плазма, Индуктивный, Геликонный, Мультикаспový, Распылительный.

Розробка ВЧ іонних джерел для прискорювачів сфокусованих іонних пучків

В.І. Возний, В.І. Мірошниченко, С.М. Мордик, Д.П. Шульга,
В.Ю. Сторіжко, В.В. Токмань

Інститут прикладної фізики, Національна академія наук України,
вул. Петропавловська, 58, 40000 Суми, Україна

Представлені результати досліджень іонних джерел, розроблених у ІПФ НАН України, для отримання високояскравісних іонних пучків з малим енергетичним розкидом. Проведено дослідження ряду іонних ВЧ-джерел, що працюють на частоті 27,12 МГц: індуктивного ВЧ-джерела, геліконового джерела, мультікаспового ВЧ-джерела та ВЧ-джерела іонів металів розпорошувального типу. Для розрахунку плазмових параметрів ВЧ-джерел розглядалася глобальна і трансформаторна моделі розряду. Проведено виміри енергетичного розкиду, масового складу та густини струму деяких джерел в широкому діапазоні ВЧ-потужності, витягаючої напруги і тиску робочого газу.

Ключові слова: ВЧ джерело іонів, Плазма, Індуктивний, Геліконий, Мультікасповий, Розпорошувальний.

REFERENCES

1. D.N. Jamieson, *7 Intern. Conference on Nuclear Microprobe Technology and Applications*, MF-01, (Bordeaux: France: 2000).
2. G.J.F. Legge, G.R. Moloney, *Rev. Sci. Instrum.* **67**, 909 (1996).
3. C. Lejeune, J. Aubert, *Advances in Electr. and Electron Physics* (New York: Septier: 1980).
4. V.I. Miroshnichenko, S.N. Mordik, *Nucl. Instrum. Meth. B* **201**, 630 (2003).
5. V.I. Voznyy, V.I. Miroshnichenko, S.M. Mordyk, A.G. Nagornyy, D.A. Nagornyy, V.E. Storizhko, D.P. Shulha, *Probl. At. Sci. Tech. Ser.: Plasma Physics* **10** No 1, 209 (2005).
6. V.I. Miroshnichenko, S.M. Mordyk, V.I. Voznyy, V.E. Storizhko, D.P. Shulha, *Nucl. Instrum. Meth. B* **260**, 39 (2007).
7. S.N. Mordyk, V.I. Vozniy, V.I. Miroshnichenko, V.E. Storizhko, D.P. Shulga, *Prikladnaya Fizika* **No 2**, 70 (2008). [in Russian]
8. V.I. Voznyy, V.I. Miroshnichenko, S.M. Mordyk, D.P. Shulha, V.E. Storizhko, *Visnyk SumDU* No 1, 28 (2008) [in Russian]..
9. V.I. Voznyi, *Visnyk SumDU* No 1, 136 (2008). [in Russian]
10. S. Mordyk, V. Miroshnichenko, D. Shulha, V. Storizhko, *Rev. Sci. Instrum.* **79**, 02B707 (2008).
11. V. Voznyi, *J. Nano-Electron. Phys.* **2** No 2, 75 (2010).
12. V.I. Voznyi, V.I. Miroshnichenko, S.N. Mordik, A.G. Nagornyi, D.A. Nagornyi, V.E. Storijko, D.P. Shul'ga, *Nauka ta Innovaciiї* **6** No5, 38 (2010). [in Russian].
13. V.I. Voznyi, V.E. Storizhko, V.I. Miroshnichenko, D.P. Shulha, *J. Nano-Electron. Phys.* **4** No 3, 03019 (2012).
14. R.B. Piejak, V.A. Godyak, B.M. Alexandrovich, *Plasma Sources Sci. Technol.* **1**, 179 (1992).
15. V.A. Godyak, R.B. Piejak, B.M. Alexandrovich *Plasma Sources Sci. Technol.* **3**, 169 (1994).
16. M.A. Lieberman, A.J. Lichtenberg, *Principles of Plasma Discharges and Materials Processing* (New York: Wiley: 1994).
17. R.W. Boswell, *Phys. Lett. A* **33**, 457 (1970).
18. F.F. Chen, *J. Vac. Sci. Technol. A* **10**, 1389 (1992).
19. K.P. Shamrai, V.B. Taranov, *Plasma Sources Sci. Technol.* **5**, 474 (1996).
20. K.P. Shamrai, V.F. Virko, *J. Vac. Sci. Technol. A* **15** No6, 2864 (1997).
21. J.T. Gudmundsson, *Plasma Sources Sci. Technol.* **8**, 58 (1999).
22. Y. Mutsuo, *Jpn. J. Appl. Phys.* **26**, 721 (1987).
23. K. Miyake, K. Ohashi, *Nucl. Instrum. Meth. B* **121**, 102 (1997).